AGU PUBLICATIONS

JGR

Journal of Geophysical Research: Atmospheres

RESEARCH ARTICLE
10.1002/2014JD021955

Key Points:
- High-resolution mass spectrometry of aerosol particles from CalNex 2010
- Comparison between two techniques shows good overlap in aerosol composition
- Observe variation in organosulfate and organonitrate composition during the day

Supporting Information:
- Readme
- Figure S1
- Figure S2
- Figure S3
- Figure S4
- Figure S5
- Figure S6
- Figure S7
- Table S1
- Table S2
- Table S3
- Table S4
- Table S5
- Table S6
- Table S7
- Table S8
- Text S1

Correspondence to:
A. Laskin and A. H. Goldstein,
Alexander.Laskin@pnnl.gov;
ahg@berkeley.edu

Citation:
O'Brien, R. E., A. Laskin, J. Laskin, C. L. Rubitschun, J. D. Surratt, and A. H. Goldstein (2014), Molecular characterization of S- and N-containing organic constituents in ambient aerosols by negative ion mode high-resolution Nanospray Desorption Electrospray Ionization Mass Spectrometry: CalNex 2010 field study, *J. Geophys. Res. Atmos.*, *119*, 12,706–12,720, doi:10.1002/2014JD021955.

Received 1 MAY 2014
Accepted 18 OCT 2014
Accepted article online 22 OCT 2014
Published online 19 NOV 2014

Molecular characterization of S- and N-containing organic constituents in ambient aerosols by negative ion mode high-resolution Nanospray Desorption Electrospray Ionization Mass Spectrometry: CalNex 2010 field study

Rachel E. O'Brien[1,2,3], Alexander Laskin[4], Julia Laskin[5], Caitlin L. Rubitschun[6], Jason D. Surratt[6,7], and Allen H. Goldstein[7,8]

[1]Department of Chemistry, University of California, Berkeley, California, USA, [2]Now at Lawrence Berkeley National Laboratory, Berkeley, California, USA, [3]Now at Department of Chemistry, University of the Pacific, Stockton, California, USA, [4]William R. Wiley Environmental and Molecular Sciences Laboratory, Pacific Northwest National Laboratory, Richland, Washington, USA, [5]Physical Sciences Division, Pacific Northwest National Laboratory, Richland, Washington, USA, [6]Department of Environmental Sciences and Engineering, Gillings School of Global Public Health, The University of North Carolina at Chapel Hill, Chapel Hill, North Carolina, USA, [7]Department of Environmental Science, Policy, and Management, University of California, Berkeley, California, USA, [8]Department of Civil and Environmental Engineering, University of California, Berkeley, California, USA

Abstract Samples of ambient aerosols from the 2010 California Research at the Nexus of Air Quality and Climate Change (CalNex) field study were analyzed using negative ion mode Nanospray Desorption Electrospray Ionization High-Resolution Mass Spectrometry (nano-DESI/MS). Four samples per day (6 h each) were collected in Bakersfield, CA on 20–24 June. Four characteristic groups were identified: molecules composed of carbon, hydrogen, and oxygen only (CHO), sulfur- (CHOS), nitrogen- (CHON), and both nitrogen- and sulfur-containing organics (CHONS). The chemical formula and elemental ratios were consistent with the presence of organonitrates, organosulfate, and nitroxy organosulfates in the negative ion mode mass spectra. The number of observed CHO compounds increased in the afternoon samples, suggesting photochemical processing as a source. The average number of CHOS compounds had the smallest changes during the day, consistent with a more broadly distributed source. Both of the nitrogen-containing groups (CHONS and CHON) had greater numbers of compounds in the early morning (midnight to 6 A.M.) and night (6 P.M. to midnight) samples, respectively, consistent with nitrate radical chemistry as a likely source for those compounds. Most of the compounds were found in submicron particles. The size distribution of the number of CHON compounds was bimodal, potentially indicating two types of sources. We conclude that the majority of the compounds observed were secondary in nature with both biogenic and anthropogenic sources. These data are complementary to previous results from positive ion mode nano-DESI/MS analysis of a subset of the same samples providing a more complete view of aerosol chemical composition at Bakersfield.

1. Introduction

Atmospheric aerosols absorb and scatter radiation and can serve as cloud condensation nuclei, thus affecting the Earth's climate [*Poschl*, 2005; *Solomon et al.*, 2007]. These effects are strongly impacted by the chemical composition of the aerosols. Organic compounds are a major fraction of atmospheric fine particulate matter ($PM_{2.5}$, aerosol with aerodynamic diameters of 2.5 μm or less), and thus, contribute to their chemical complexity [*Kanakidou et al.*, 2005; *Fuzzi et al.*, 2006; *Zhang et al.*, 2007; *Williams et al.*, 2010]. Secondary organic aerosol (SOA) contribute a large fraction toward the organic material found in $PM_{2.5}$ and are formed by the condensation of low-volatility organic compounds and subsequent particle phase and gas-particle reactions [*Seinfeld and Pankow*, 2003; *Ervens et al.*, 2011]. Identifying the chemical composition of the organic fraction is necessary to advance our understanding of the sources, chemical transformation processes, and the environmental impacts of aerosols.

The complexity of organic aerosols is greatly increased by the addition of nitrogen and sulfur through processes including gas phase, condensed-phase, and heterogeneous gas-particle reactions. Nitrogen-containing

compounds such as organonitrates have been found to comprise 10–20% of the aerosol organic mass fraction [*Zhang et al.*, 2002; *Holzinger et al.*, 2010]. Two potential mechanisms for the formation of organonitrates include the reaction of alkenes with NO_3 radicals at night and the daytime reaction of NO with organic peroxy radicals under high NO_x conditions [*Roberts*, 1990; *Gong et al.*, 2005; *Ng et al.*, 2008]. Sulfur-containing compounds, such as organosulfates, have also been reported to make up a large portion (30%) of the organic mass fraction in certain locations [*Surratt et al.*, 2008]. Multiple mechanisms for the formation of organosulfates have been proposed, including reactive uptake of gaseous epoxides onto acidic aerosols [*Iinuma et al.*, 2009; *Surratt et al.*, 2010; *Zhang et al.*, 2012] and radical-initiated formation driven by photochemistry of sulfate ions [*Noziere et al.*, 2010].

Traditionally, gas chromatography interfaced with mass spectrometry (GC/MS) has been used to measure the chemical composition of the organic fraction in fine aerosol samples. This technique is well suited for the characterization of low molecular weight organic compounds found in aerosols, but typically only 10–30% of the organic mass is identified at the molecular level [*Rogge et al.*, 1993]. High-molecular weight and polar compounds comprise a large portion of organic aerosols and are generally not measureable with GC-MS [*Havers et al.*, 1998; *Samburova et al.*, 2005; *Kalberer*, 2006]. Electrospray ionization (ESI) [*Fenn et al.*, 1990], combined with high-resolution mass spectrometry is an effective tool to probe the molecular composition of complex atmospheric samples [*Nizkorodov et al.*, 2011; *Laskin et al.*, 2012]. The use of high-resolution mass spectrometry allowed identification of thousands of organic compounds including organosulfates, organonitrates, and nitroxy organosulfates in aerosol, fog, and rainwater samples [*Reemtsma et al.*, 2006; *Altieri et al.*, 2009; *Mazzoleni et al.*, 2010; *Lin et al.*, 2012a; *Nguyen et al.*, 2012; *Kourtchev et al.*, 2013]. From the differences in the composition of ambient organic aerosols collected over different periods of time, insights into the sources and chemical transformations of aerosols can be obtained [*O'Brien et al.*, 2013a, 2013b].

A novel ambient pressure ionization technique, Nanospray Desorption Electrospray Ionization combined with High-Resolution Mass Spectrometry (nano-DESI/MS) [*Roach et al.*, 2010b], has been introduced for the analysis of organic aerosol samples [*Roach et al.*, 2010a]. In nano-DESI, the analyte is quickly dissolved from the surface of the substrate and ionized directly in front of the instrument inlet. This technique limits potential solvent-analyte interactions that can occur with the typical solvent extraction done for ESI analysis [*Laskin et al.*, 2010]. Nano-DESI has been shown to be a powerful technique for the analysis of complex mixtures on substrates with improved preservation of some labile functional groups and minimal sample preparation [*Roach et al.*, 2010a].

The data set presented here is complementary to the positive ion mode data set from 22 to 23 June discussed in our previous study [*O'Brien et al.,* 2013a, 2013b]. Data in the positive ion mode consisted of CHO and CHON compounds and the number of compounds in each group was analyzed as a function of time of day. Trends observed were consistent with a photochemistry/ozonolysis source for CHO compounds and the formation of reduced nitrogen-containing compounds through imidization reactions [*O'Brien et al.*, 2013a]. Potential sources for SOA in Bakersfield were investigated by comparing ambient molecular formulas with the formulas from aerosols generated in a smog chamber. The overlap in molecular formulas between diesel SOA and the ambient samples was larger than for isoprene SOA indicating that diesel was likely a contributing source for aerosols in Bakersfield [*O'Brien et al.*, 2013b]. Ionization in positive mode favors compounds that can easily be protonated such as alcohols, amines, etc. Here the negative ion mode mass spectra provide complementary information on the CHO and CHON classes of compounds. Negative ion mode favors the ionization of compounds that can be easily deprotonated such as carboxylic acids, organosulfates, organonitrates, etc.

In this study, the chemical characterization of the organic fraction of aerosols collected over 20–24 June in Bakersfield California during the CalNex 2010 field study is reported. We used the nano-DESI/MS analytical platform in negative ion mode to probe substrate-deposited, size-resolved aerosol samples and assigned molecular formulas for over 1000 organic compounds detected in the samples. We report differences in the aerosol composition during the day across four classes of organic compounds with characteristic composition of CHO, CHON, CHOS, CHONS, and complement molecular formulas with organosulfates and nitroxy organosulfates probed by ultraperformance liquid chromatography interfaced to ESI HR quadrupole time-of-flight mass spectrometry (UPLC/ESI-HR-Q-TOFMS) in concurrent $PM_{2.5}$ samples. We also report diurnal trends in the variations of organic compounds observed in the size-resolved samples.

2. Experimental

2.1. Sample Collection and Chemical Analysis

2.1.1. Nano-DESI/HRMS

Samples of ambient aerosols were collected in Bakersfield, California (35.35°N, 118.97°W) during the CalNex field study. A detailed description of the meteorology, field site, and sampling techniques are provided elsewhere [*O'Brien et al.*, 2013a]. Briefly, samples collected on 20–24 June were chosen for in-depth analysis based on real-time concurrent measurements at the sampling site. Time-of-flight aerosol mass spectrometry and in situ thermal desorption aerosol gas chromatography indicated high SOA loadings and characteristic diurnal patterns similar to the rest of the campaign. The meteorology on these days was characteristic of the entire campaign and included higher ozone and air temperatures (25–35°C) during the afternoon and higher relative humidity at night (40–70% relative humidity). The sun rose at approximately 6 am and set at 7 pm PDT.

Aerosol samples were collected for six hours using a micro-orifice uniform deposit impactor (MOUDI) model 100R (MSP, Inc.) without rotation on aluminum foil substrates. Four samples were collected for each day: early morning (midnight to 6 A.M.), morning (6 A.M. to noon), afternoon (noon to 6 P.M.) and night (6 P.M. to midnight). Samples on the eighth stage of the MOUDI (0.18–0.32 μm aerodynamic diameter (D_a)) had the highest mass loadings and were chosen for intensive study. A 12 h sample was acquired on 24 June from noon to midnight, and stages 8 to 5 ($0.18 < D_a < 1.8$ μm) were analyzed to provide size-resolved data. All times are reported as local time (PDT) and samples were stored at −80°C until analysis.

Aerosol samples were analyzed in the Environmental Molecular Sciences Laboratory located at Pacific Northwest National Laboratory (PNNL). A high-resolution LTQ-Orbitrap MS (Thermo Fisher, Bremen, Germany) with a custom built nano-DESI source was used for the analysis. The source consists of two fused-silica capillaries (193 μm o.d. /50 μm i.d, Polymicro Technologies LLC, Phoenix, AZ). The primary capillary delivers acetonitrile solvent to the sample while the secondary, nanospray, capillary removes the analyte mixture desorbed into the solvent and transfers it to a mass spectrometer inlet. The solvent flow rate is adjusted to form a droplet on the surface of the substrate. Electrospray was maintained at a flow rate of 1.0−2.0 μL/min and a voltage of ~6 kV applied to a stainless steel union holding the tip of the primary capillary. The instrument was operated in the negative ion mode with a resolution of 60,000 m/Δm at 400 m/z. The instrument was externally calibrated using a standard ESI calibration mix of sodium dodecylsulfate, sodium taurocholate, MRFA (peptide), caffeine, and Ultramark 1621.

2.1.2. UPLC/ESI-HR-Q-TOFMS

Twenty-three hour integrated fine aerosol samples were collected from 19 May to 26 June onto prebaked quartz fiber filters (Pall Life Sciences, 102 mm) using a high-volume filter sampler operated at 226 L min^{-1} and equipped with a $PM_{2.5}$ cyclone in order to provide additional samples for complimentary UPLC/ESI-HR-Q-TOFMS analysis at UNC. Only those samples that overlap with the nano-DESI/MS samples described above are presented here. The samples were stored in a freezer at −20°C until analysis. Weekly field blanks were collected by placing prebaked quartz fiber filters into the samplers for 15 min. Detailed filter extraction procedures can be found in *Lin et al.* [2013]. Briefly, precleaned scintillation vials with 15 mL high-purity methanol (LC-MS Chromasolv Grade, Sigma-Aldrich) and 45 min of ultrasonication were used for extraction. Resultant extracts were filtered to remove quartz filter fibers and insoluble particles. The extracts were dried under a gentle N_2 gas stream. The residues were immediately reconstituted with 250 μL of a 1:1 (v/v) solvent mixture of 0.1% acetic acid in water (LC-MS Chromasolv grade, Sigma-Aldrich) and 0.1% acetic acid in methanol (LC-MS Chromasolv grade, Sigma-Aldrich). Samples were agitated and sonicated for 5 min before storage at −20°C. The field and lab blanks were treated similarly and none of the compounds discussed here were observed in the blanks.

Chemical characterization of $PM_{2.5}$ was performed by injecting 5 μL of each filter extract into an ultra performance liquid chromatographic system (Waters ACQUITY) interfaced to a high-resolution quadrupole time-of-flight mass spectrometer (Agilent 6500 Series). This instrument is equipped with an ESI source (UPLC/ESI-HR-Q-TOFMS) operated in the negative (–) ion mode. Chromatographic separations were performed using a Waters ACQUITY UPLC HSS T3 column (2.1 × 100 mm, 1.8 μm particle size) operated at 45° C. Detailed UPLC/(–)ESI-HR-Q-TOFMS operating conditions and calibration procedures can be found in *Zhang et al.* [2011]. Briefly, the resolving power was set at ~9000 m/Δm, which allows for accurate mass measurements and subsequent elemental compositions of observed negative ions to be determined.

2.2. Data Analysis

2.2.1. Nano-DESI/HRMS

Nano-DESI/MS spectra were analyzed using similar techniques as previous studies [*Nguyen et al.*, 2010; *Nizkorodov et al.*, 2011; *O'Brien et al.*, 2013a. 2013b]. Briefly, raw mass spectra were obtained over the edge of the substrate that did not have impacted particles (blank MS) and over areas with impacted particulate matter (sample MS). Peaks in the mass spectra with a signal-to-noise ratio higher than 3 were extracted. Peaks in the sample MS with intensities less than 10 times that of the blank MS were removed from the analyzed data. Molecular assignments were obtained using MIDAS molecular formula calculator (http://magnet.fsu.edu/~midas/) using the following ranges: $C_{1-100}H_{0-200}O_{0-50}N_{0-3}S_{0-1}$. To assign the molecular formulas of higher mass peaks, Kendrick analyses [*Kendrick*, 1963] were used with $C_3H_4O_2$ and oxygen as bases, and a mass defect analysis of the second order using CH_2 and H_2 bases [*Roach et al.*, 2011]. Approximately 65–80% of the peaks were unambiguously assigned molecular formulas. The unassigned peaks were further checked for assignments with $S > 1$ but no matches were found. Compounds were observed as deprotonated molecules and the mass of the neutral species was obtained by adding the mass of a proton to the measured *m/z*. Since each compound may have multiple isomers, the number of compounds discussed above reflects only the number of unique molecular formulas observed while the number of unique molecular structures is substantially larger. Therefore, the term "compound" in this paper refers to all of the molecules sharing the same molecular formula. Double bond equivalence values (DBE) provide information on the number of rings and double bonds in the molecules. DBE were calculated using equation (1):

$$\mathrm{DBE} = 1 + c\text{–}h/2 + n/2 \tag{1}$$

where *c*, *h*, and *n* correspond to the number of carbon, hydrogen, and nitrogen atoms in the molecular formula, respectively. The aromaticity index (AI) is a useful way to characterize the extent of aromaticity in atmospheric organic matter [*Koch and Dittmar*, 2006; *Bateman et al.*, 2009]. AI values for the compounds were calculated using equation (2):

$$\mathrm{AI} = (1 + \mathrm{c} - \mathrm{o} - \mathrm{s} - (0.5\ \mathrm{h}))/(\mathrm{c} - \mathrm{o} - \mathrm{s} - \mathrm{n})\ \ (= 0\ \ \mathrm{if}\ \ \mathrm{negative}) \tag{2}$$

While there are exceptions, in general, AI values greater than 0.5 indicate the presence of aromatic rings and values ≥ 0.67 are characteristic of condensed aromatic structures [*Koch and Dittmar*, 2006].

2.2.2. UPLC/ESI-HR-Q-TOFMS

Mass spectral data acquired by the UPLC/ESI-HR-Q-TOFMS (UPLC/MS, hereafter) were analyzed using Mass Hunter Version B.03.01 Build 3.1.346.0 software (Agilent Technologies). Compounds observed by UPLC/MS analysis were primarily organosulfates and nitroxyorganosulfates derived from biogenic volatile organic compounds (BVOCs), as described previously in *Surratt et al.* [2008]. Commercial standards are not available for any of these compounds for quantification. Thus, calibration curves of propyl sulfate (City Chemical, 98% purity), octyl sulfate (Sigma, 99% purity), and decyl sulfate (Fluka, 99% purity) were used as surrogate standards. All three contain an organosulfate group ($R\text{-}OSO_3$); therefore, their response factor during UPLC/MS analyses should be similar to those of the measured organosulfates and nitroxyorganosulfates. The calibration responses for the octyl and decyl sulfate surrogate standards only differed by a factor of ~1.4, whereas these more hydrophobic surrogate organosulfates were ~10 times more responsive than propyl sulfate at the same concentrations. This behavior can be explained by the fact that the octyl and decyl sulfates eluted at later retention times where the mobile phase was composed of a larger percentage of volatile methanol, which allows these compounds to become more surface active on ESI droplets and thus more readily ionized. Propyl sulfate eluted earlier in the reverse-phase chromatographic runs when water composed the largest fraction of the mobile phase composition, and thus, the ESI droplets were not as conducive in producing ions for this standard. This behavior is noted here as differences between organosulfates responses could be as large as a factor of 10, thus providing some insights for the quantification uncertainty of organosulfates actually present in the ambient samples. One of these three surrogate standards was chosen to quantify these compounds on the basis of retention time (RT) and structural similarity (i.e., similar carbon numbers). Extraction efficiency as determined by analyzing blank filters spiked with the surrogate standards ranged from 73 to 76% and a constant correction factor of 75% was applied. Corrections for the quantity of filter extracted were made, and all reported concentrations and abundances are for the entire 102 mm prebaked quartz filter.

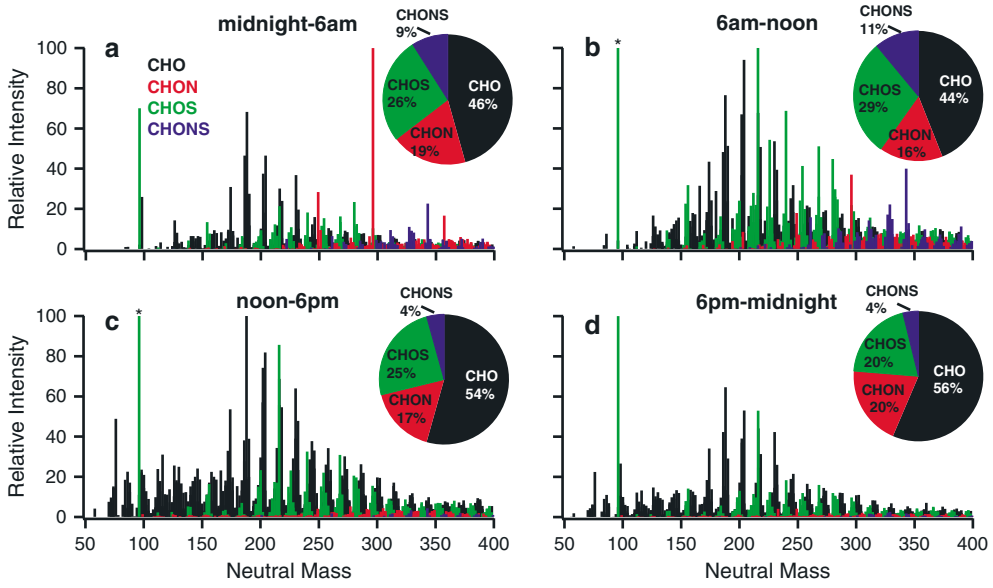

Figure 1. Negative mode mass spectra for the identified peaks in the four samples collected on 23 June from the nano-DESI/MS analysis. Pie charts show the percentage of compounds in each class at different times of day averaged over 4 days. The starred peaks at 95.988 D_a in Figure 1b and 1c have relative intensities of 161 and 231, respectively, on this scale.

3. Results and Discussion

3.1. Sample Comparison

Sixteen samples were collected over four consecutive days (20–23 June) during CalNex 2010 in Bakersfield, CA. Using negative ion mode nano-DESI/MS, the molecular formulas of ~600–900 compounds were identified in the mass range of 50–400 Da for each sample. Figure 1 shows representative mass spectra for the identified compounds from 23 June samples; spectra for the other samples are given in Figures S2–S4 in the supporting information. The compounds fall into four main groups: carbon, hydrogen, and oxygen only (CHO); nitrogen-containing (CHON); sulfur-containing (CHOS); and compounds that contain both nitrogen and sulfur (CHONS). The pie charts show the percentage of compounds measured in each category. The data in the pie charts are averaged over the 4 days; the data for each day individually are given in Table S1. There was some variability in the trends observed throughout the day across the 4 days analyzed, likely due to either differences in meteorology, sources/processing, or ionization and detection variations in the measurement technique. The following discussion will highlight trends with data points outside of the standard deviation of the other samples. However, the data set presented here covers only a small number of days and a substantially larger data set would be necessary to determine the statistical significance of the observed variations. Approximately 44–56% of the compounds were CHO with greater numbers of peaks in the afternoon and night samples although only the night (6 P.M. to midnight) and early morning (midnight to 6 A.M.) samples were outside of one standard deviation of each other. Some of the increase is due to the increased numbers of lower mass ($<$125 D_a) CHO compounds in the afternoon and night samples. Larger amounts of CHO compounds in the afternoon is consistent with results from positive ion mode data which showed higher numbers of CHO compounds in the noon–midnight samples on 22 and 23 June [*O'Brien et al.*, 2013a]. Approximately 20–29% of the compounds were CHOS and the majority of these compounds were found at the higher end of the mass scale ($>$200 D_a). The peak at 95.988 Da is CH_4O_3S which is the molecular formula for methansulfonic acid. With electrospray ionization, the observed intensities depend on the ionization efficiency, the solution composition, and the concentration of the compound. Thus, the high intensity of the peak is likely due to its high ionization efficiency although the possibility of higher concentrations of this compound cannot be ruled out. The number of CHON compounds ranged from approximately 16 to 20%, and on average, the percentages were highest at night and in the early morning, although only the night (6 P.M. to midnight) and morning (6 A.M. to noon) samples were outside of one standard deviation of each other. The remaining 4–11% of the compounds were CHONS compounds. Greater

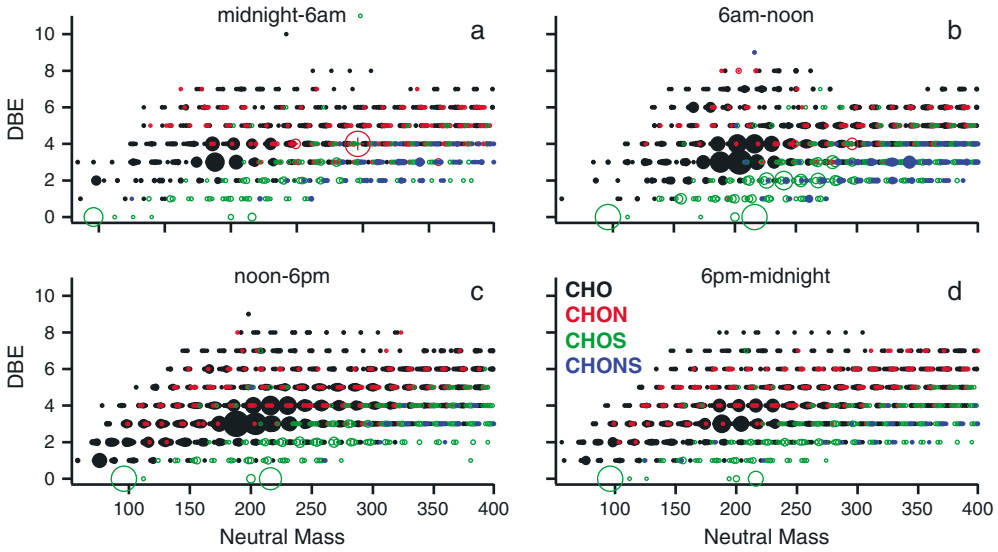

Figure 2. DBE plots for the samples collected on 23 June from the nano-DESI/MS analysis. The size of the markers is proportional to the peak intensity. The CHON (red) and CHOS (green) data points in Figure 2b are shown as open circles.

numbers of CHONS compounds were observed in the early morning and morning samples (midnight to 6 A.M. and 6 A.M. to noon) than in the night sample (6 P.M. to midnight).

In the samples discussed above, the sulfur and nitrogen in CHON, CHOS, and CHONS compounds are assumed to be covalently bound. To distinguish between covalently bound and weak noncovalent complexes of $[M + HSO_4]^-$ or $[M + NO_3]^-$ that could be formed in electrospray and would have the same CHON and CHOS elemental composition, in-source collision-induced dissociation (CID) was performed. In these experiments ions are accelerated by a 30 V field gradient in the presence of collision gas resulting in efficient dissociation of noncovalent complexes [*Duffin et al.*, 1991] while a majority of ions with covalently bound structures stay intact. The sample collected on 24 June midnight to 6 A.M. was analyzed for stability of CHOS, CHON, and CHONS compounds during the in-source CID experiments. For compounds that had MS peaks >5% relative intensity (RI), more than 82% of the compounds in each group remained after CID (Table S2). This suggests that the amount of noncovalent complexes was very small. We note that the majority (~72–97%), of the CHOS, CHONS, and CHON compounds are low-intensity peaks with RI values less than 5%. Since noncovalent complexes are likely to dissociate with CID, the loss of a compound in the mass spectra after CID raises the possibility that the compound is not covalent. However, since there is a natural variability of peak intensities as the samples are collected, caution must be used when comparing the low-intensity peaks in different samples in a CID analysis since their loss during a CID analysis may simply be due to changes in the population of compounds ionized as the sample is raster scanned. Our results indicate that a majority of the observed CHOS, CHONS, and CHON compounds were stable covalently bound species.

3.2. Characterization by Group

3.2.1. CHO Compounds

Between 208 and 542 compounds were assigned CHO molecular formulas for each sample. More CHO compounds were observed in the afternoon and night samples than the rest of the day and the number of CHO compounds observed in the night samples (6 P.M. to midnight) was outside of the standard deviation of the early morning and morning samples (Figure 1). The same trend was observed for the positive mode data and the increased abundances have been attributed to photochemistry and ozonolysis [*O'Brien et al.*, 2013a]. In Figure 1, the CHO compounds, shown in black, cover a wide range of masses from 50 to 400 Da. The mass spectra peaks with the highest intensity are centered around 150–300 Da. *Reemtsma et al.* [2006] found the highest intensity CHO peaks in a similar *m/z* range in an analysis of aerosol samples collected in Riverside, CA. Aerosol samples collected in New York (NY) and Virginia (VA) showed a slightly higher range of ~230–350 for the most abundant peaks [*Wozniak et al.*, 2008]. Aerosol samples collected in the Pearl River Delta Region, China, had slightly lower maximum intensities between ~50 and 250 Da [*Lin et al.*, 2012a]. In Figure 2, DBE

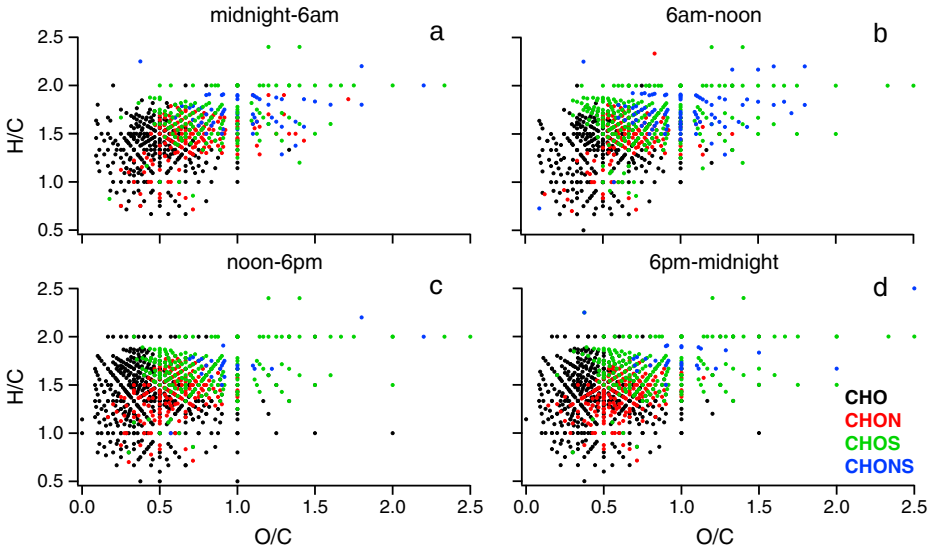

Figure 3. Van Krevelen diagrams for the four samples collected on 23 June from the nano-DESI/MS analysis. The H:C versus the O:C values for each identified compound are shown broken down by group.

values are plotted against the neutral mass for the same sample, 23 June. The CHO compounds cover a range of DBE values of 1–8. This is similar to the CHO compounds measured in the positive mode in samples collected on 23 June at Bakersfield which had DBE = 2–10 for the majority of the CHO compounds observed [*O'Brien et al.*, 2013a]. AI values indicated that there were between 4 and 26 CHO compounds with an aromatic ring in each sample with slightly more, on average, in the afternoon and night samples (noon–midnight) (Table S3). In most of the samples there were also a few compounds (up to 10) with AI $\geq$ 0.67 indicating the presence of condensed aromatic compounds [*Koch and Dittmar*, 2006].

Additional insight into changes in the chemical composition of the aerosol throughout the day can be gained by examining the elemental ratios of each group. In Figure 3, Van Krevelen diagrams are shown for the 23 June samples. The majority of the CHO compounds, shown in black, fall between $0.5 < H/C < 2.0$ and $0.1 < O/C < 1.0$. These are similar to the ranges previously reported for CHO compounds in aerosols, rainwater, and fog [*Altieri et al.*, 2009; *Mazzoleni et al.*, 2010; *Lin et al.*, 2012a; *Kourtchev et al.*, 2013]. The range is also comparable to aerosol samples collected in NY and VA except that the O/C range here extends to higher values (0.6 versus 1.0) [*Wozniak et al.*, 2008]. In Table 1, the intensity weighted average elemental ratios are shown, averaged over the 4 days. The average ratios for each sample individually are given in Table S4. The <H/C> value increases from 1.4 to 1.5 and the <O/C> value drops from 0.55 to about 0.5 going from the early morning (midnight to 6 A.M.) to the afternoon and night (noon to 6 P.M. and 6 P.M. to midnight) samples. The morning sample

Table 1. Average Elemental Ratios for Each Compound Group Averaged Over 4 Days From the Nano-DESI/MS Analysis (20–23 June)[a]

		Midnight to 6 A.M.	6 A.M. to Noon	Noon to 6 P.M.	6 P.M.to Midnight
<O/C>	CHO	0.55 ± 0.02	0.55 ± 0.06	0.49 ± 0.02	0.50 ± 0.02
	CHON	0.78 ± 0.08	0.73 ± 0.03	0.62 ± 0.01	0.64 ± 0.01
	CHOS	0.87 ± 0.09	0.93 ± 0.1	0.82 ± 0.09	0.88 ± 0.05
	CHONS	0.99 ± 0.02	1.0 ± 0.005	0.92 ± 0.03	0.89 ± 0.09
<H/C>	CHO	1.4 ± 0.0	1.4 ± 0.08	1.5 ± 0.05	1.5 ± 0.05
	CHON	1.5 ± 0.0	1.5 ± 0.05	1.5 ± 0.0	1.5 ± 0.05
	CHOS	1.7 ± 0.05	1.8 ± 0.1	1.8 ± 0.05	1.8 ± 0.0
	CHONS	1.7 ± 0.0	1.7 ± 0.0	1.7 ± 0.05	1.7 ± 0.05
<N/C>	CHO	-	-	-	-
	CHON	0.13 ± 0.01	0.13 ± 0.06	0.085 ± 0.003	0.089 ± 0.004
	CHOS	-	-	-	-
	CHONS	0.11 ± 0.008	0.12 ± 0.006	0.11 ± 0.02	0.10 ± 0.01

[a]The standard deviations of the four data sets are given.

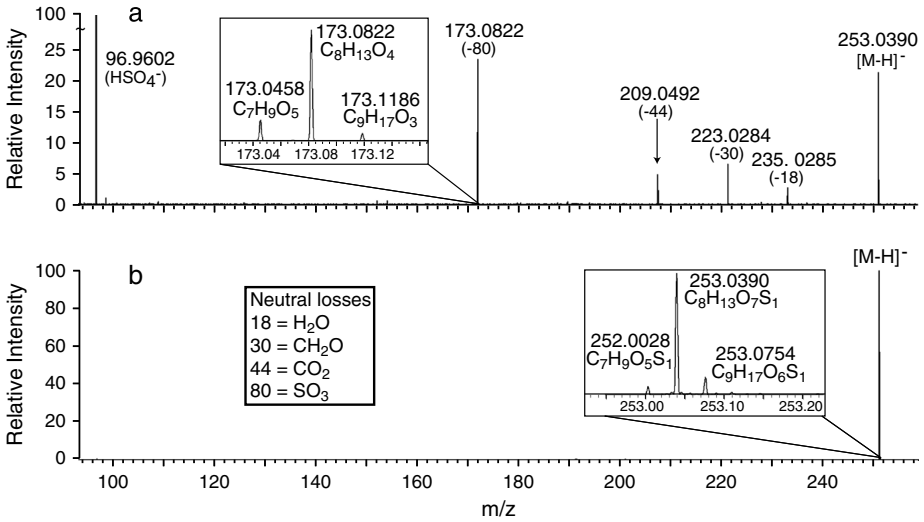

Figure 4. MS/MS of CHOS compounds from 21 June midnight to 6 A.M. sample from the nano-DESI/MS analysis. (a) Product ion mass spectra and (b) precursor mass spectra with ionization window 0.1 Da.

(6 A.M.to noon) has similar <H/C> and <O/C> values as the early morning sample (midnight to 6 A.M.). However, the standard deviation of those values for the morning sample is within the uncertainty of the samples from the other time periods. The increase in <H/C> and decrease in <O/C> are also observed in Figure 3 as an increased number of peaks in the upper left section of the Van Krevelen diagram covered by CHO compounds. The changes suggest that the fresh CHO compounds in the afternoon and night samples are less oxidized and more saturated than the compounds observed in the early morning samples. This is also observed in Figure 2 with more CHO compounds at lower DBE values in the afternoon and night samples, especially in the lower mass region. The CHO compounds measured in Bakersfield have similar elemental ratios and compositions to CHO compounds measured in other atmospheric samples [*Reemtsma et al.*, 2006; *Wozniak et al.*, 2008; *Altieri et al.*, 2009; *Mazzoleni et al.*, 2010] and the increased number of compounds in the afternoon suggests daytime production by photochemistry and ozonolysis. The increased oxidation in the early morning samples suggests that the compounds in the aerosols formed during the day may continue to oxidize either heterogeneously or homogenously. A few compounds had <H/C> and/or <O/C> values outside of the axis limits in the van Krevelen diagrams, they are listed in Table S5. The majority of these compounds have small numbers of carbon atoms and large numbers of oxygen atoms and/or hydrogen atoms. The increased <O/C> values of these compounds are likely due to the presence of sulfate and nitrate groups. The remaining compounds are likely either fragments (CH_4O_3) or have low H/C values and are likely aromatic.

3.2.2. CHOS

The majority of the CHOS compounds, displayed in green, were located at higher H/C and O/C values than the CHO compounds (Figure 3 and Table 1). The average molecular weights were higher for the CHOS compounds (Figure 1) and more than 96.5% of the compounds measured in each sample had O/S values greater than 4. All of these observations are consistent with the majority of the sulfur atoms occurring in sulfate groups. A few of the CHOS compounds were isolated and product ion mass spectra were generated, an example is shown in Figure 4. Losses of 79.9568 Da ($-SO_3$) and the occurrence of 96.9620 (HSO_4^-) were observed in all of the product mass spectra and provide further evidence for the assignment of organosulfates [*Reemtsma et al.*, 2006]. The majority of the CHOS compounds have DBE values that range from approximately 0 to 4 (Figure 2), lower than the CHO compounds discussed above. Low DBE or high H/C values for organosulfate compounds were also observed in fog, rainwater, and aerosol samples [*Reemtsma et al.*, 2006; *Wozniak et al.*, 2008; *Altieri et al.*, 2009; *Mazzoleni et al.*, 2010; *Lin et al.*, 2012b].

There were between 126 and 253 CHOS compounds detected and the CHOS compounds show the smallest variation in diurnal pattern over the 4 day averages (Figure 1 and Table S1). Either the main source for these compounds was remote from the sampling site, or the number of compounds observed did not strongly depend on the meteorology at the site. The elemental ratios of the CHOS compounds were compared to the ratios for organosulfates formed from the gas phase oxidation of isoprene, α-pinene, β-pinene,

Table 2. Organosulfate Compounds Detected With Both UPLC/MS and Nano-DESI/MS Analysis

		Concentration in ng/m^3 With UPLC/MS[a]			
Mass	Formula	20 June	21 June	22 June	23 June
139.9779	$C_2H_3O_5S_1$	0.069 (b and c)	0.000 (-)	0.000 (a and c)	0.000 (b–d)
153.9936	$C_3H_5O_5S_1$	0.064 (a–d)	0.144 (a–d)	0.081 (a–d)	0.15 (a–d)
155.9729	$C_2H_3O_6S_1$	0.019 (a–d)	0.039 (a–d)	0.019 (a–d)	0.085 (a–d)
169.9885	$C_3H_5O_6S_1$	0.045 (a–d)	0.107 (a, c, and d)	0.056 (a–c)	0.118 (a–d)
199.9991	$C_4H_7O_7S_1$	0.129 (a–d)	0.301 (a, c, and d)	0.319 (a–d)	0.528 (a–d)
211.9991	$C_5H_7O_7S_1$	0.067 (a–d)	0.000 (a, c, and d)	0.125 (a–d)	0.000 (a–d)
214.0147	$C_5H_9O_7S_1$	0.048 (a–d)	0.114 (a, c, and d)	0.118 (a–d)	0.104 (a–d)
216.0304	$C_5H_{11}O_7S_1$	0.387 (a–d)	1.104 (a, c, and d)	1.157 (a–d)	1.691 (a–d)
224.0355[b]	$C_7H_{11}O_6S_1$	0.000 (-)	0.314 (-)	0.273 (c and d)	0.391 (a–d)
227.994	$C_5H_7O_8S_1$	0.000 (a–d)	0.140 (a–d)	0.000 (a–d)	0.165 (a–d)
238.0511	$C_8H_{13}O_6S_1$	0.121 (a–d)	0.036 (b–d)	0.109 (a–d)	0.036 (a–d)
250.0511	$C_9H_{13}O_6S_1$	0.034 (a–d)	0.012 (a–d)	0.000 (a–d)	0.000 (b–d)
250.0875	$C_{10}H_{17}O_5S_1$	0.020 (a–d)	0.025 (a, c, and d)	0.000 (a and c)	0.040 (c)
252.0668	$C_9H_{15}O_6S_1$	0.058 (a, b, and d)	0.084 (d)	0.147 (a–d)	0.110 (a–d)
254.046	$C_8H_{13}O_7S_1$	0.064 (a–d)	0.095 (a–d)	0.000 (a–d)	0.000 (a–d)
266.0824	$C_{10}H_{17}O_6S_1$	0.000 (a–d)	0.000 (a–d)	0.000 (a–d)	0.000 (a–d)
268.0617	$C_9H_{15}O_7S_1$	0.092 (a–d)	0.137 (a–d)	0.071 (a–d)	0.152 (a–d)
280.0617	$C_{10}H_{15}O_7S_1$	0.106 (a–d)	0.126 (a, b, and d)	0.076 (a–d)	0.122 (a–d)
282.0773	$C_{10}H_{17}O_7S_1$	0.032 (a–d)	0.043 (a, b, and d)	0.036 (a–d)	0.067 (a–d)
284.0566	$C_9H_{15}O_8S_1$	0.007 (a–d)	0.000 (a–d)	0.000 (a–d)	0.000 (a–d)
284.093[b]	$C_{10}H_{19}O_7S_1$	0.000 (a–d)	0.013 (-)	0.000 (a and b)	0.000 (-)
298.0722	$C_{10}H_{17}O_8S_1$	0.012 (a–d)	0.000 (a–d)	0.108 (a–d)	0.022 (a–d)

[a]These organosulfates were also reported in *Surratt et al.* [2008] The first number given is the concentration in ng/m^3 found with UPLC/MS and the letters in parenthesis correspond to the time of day the elemental formula was observed in the nano-DESI/MS analysis (a = midnight to 6 A.M., b = 6 A.M. to noon, c = noon to 6 P.M., and d = 6 P.M. to midnight).
[b]Compounds observed only with UPLC/MS.

α-terpinene, γ-terpinene, and limonene [*Surratt et al.*, 2008]. Twenty-two organosulfates were observed in 23 h integrated filter samples analyzed by UPLC/MS. All of the compounds with the same elemental formulas as the organosulfates identified by UPLC/MS were observed in the nano-DESI/MS aerosol samples (Table 2). The overlap between the two measurements was very good; in 97% of the cases where an organosulfate was reported using UPLC/MS, a compound with the same molecular formula was observed by the nano-DESI/MS in at least one sample collected the same day. The recently characterized isoprene epoxydiol (IEPOX)-derived organosulfate [*Surratt et al.*, 2010; *Y.-H. Lin et al.*, 2012], which is detected as the $[M–H]^-$ ion at *m/z* 215, was found to be the most abundant (i.e., 1.7 ng m^{-3}) of the organosulfates observed by the UPLC/MS technique.

Previous work by *Lin et al.* [2012b] investigated the prevalence of the epoxide formation pathway for organosulfates and nitrooxy organosulfates by examining the presence of precursor-product pairs of the CHOS (or CHONS) and the corresponding CHO (CHON) compounds. If the epoxides form, both sulfate and water can act as nucleophiles and thus, both the organosulfate and the corresponding alcohol should be present [*Lin et al.*, 2012b]. In Table 3, a similar analysis shows that on average, over the four sample days,

Table 3. Precursor-Product Pairs for Epoxide Formation of Organosulfates and Hydrolysis Reactions From the Nano-DESI/MS Analysis[a]

	Number and Percentages of Precursor-Product Pairs		
Sample time	CHOS ➔ CHO ($-SO_3$)	CHONS ➔ CHON ($-SO_3$)	CHONS ➔ CHOS ($+OH, -NO_3$)
Midnight to 6 A.M.	77 (45%)	17 (30%)	43 (74%)
6 A.M. to Noon	70 (41%)	17 (27%)	53 (79%)
Noon to 6 P.M.	115 (63%)	12 (41%)	26 (75%)
6 P.M. to Midnight	131 (79%)	10 (30%)	22 (66%)

[a]Numbers and percent of CHOS and CHONS compounds with corresponding CHO, CHON, and CHOS formulas in the same mass spectra for the following reactions: $C_xH_yO_zS \rightarrow C_xH_yO_{z-3} + SO_3$; $C_xH_yO_zN_wS \rightarrow C_xH_yO_{z-3}N_w + SO_3$; $C_xH_yO_zN_wS \rightarrow C_xH_{y+1}O_{z-2}N_{w-1}S - H_2O + HNO_3$. Values are averaged over all four sample days.

between ~40 and 80% of the CHOS peaks had corresponding CHO formula in the sample with higher percentages in the afternoon and night samples. Results from each day individually are given in Table S6. A large part of the increase in the afternoon and night samples is likely due to the fact that there are larger numbers of CHO compounds in the afternoon and night samples. The early morning and morning values are slightly lower than what was observed in the Pearl River Delta Region of China [*Lin et al.*, 2012b] while the afternoon and night values are in the same range. These results suggest that the epoxide formation pathway on biogenic precursors is an important formation mechanism for the organosulfate compounds observed in Bakersfield.

3.2.3. CHON

The majority of the O/C values measured for the CHON compounds (red markers) fall to the right, but within the range, of the values measured for the CHO compounds (Figure 3). On average, more than 98% of the CHON compounds in each sample had O/N $>$ 3. The higher oxidation level of these compounds suggests that for the majority of them the nitrogen could be present in a nitrate (ONO_2) group. Compounds containing C, H, O, and either one, or two, or three nitrogen atoms (N1, N2, N3) in their molecular formula were observed. Almost all occurrences of N2 and N3 compounds were observed in the early morning and morning samples (midnight to 6 A.M. and 6 A.M. to noon). The CHON compounds covered a wide range of masses with averages around 280 Da. In these samples the CHON compounds had low relative intensities; on average $>$97% of the peaks had RI values below 5% (Figure 1). The majority of these compounds have DBE values between 4 and 6 (Figure 2). This is within the range of DBE values of 3–11 reported for CHON in fog water [*Mazzoleni et al.*, 2010] and is slightly higher than the range of 3–4 reported for the major components of the CHON compounds in aerosol samples collected during the SOAR campaign in Riverside, CA [*Reemtsma et al.*, 2006]. One data point in Figure 2b is outside the vertical axis limits. This compound has a formula $C_{24}H_{21}O_3N$, a neutral mass of 371.15214 Da, a DBE of 15, and is likely a condensed aromatic compound with a nitrogen atom. A small number (0–4) of CHON compounds in each sample had AI values $>$ 0.5 and $\geq$0.67 indicating the presence of aromatic rings and condensed aromatic structures (Table S3). The majority of the aromatic compounds had O/N$\leq$3. The first sample, 20 June 20 midnight to 6 A.M., had 12 compounds with AI values $\geq$0.67 and all of these had O/N$\leq$1 consistent with N-heteroatom aromatic compounds, a compound class which has been previously observed in biomass burning samples [*Laskin et al.*, 2009]. Additionally, all of the samples have molecular formula that match at least one of the three nitrocatechols reported by *Claeys et al.* [2012] in biomass burning samples.

Between 101 and 164 CHON compounds were observed, over the 4 day average, with slightly higher percentages, on average, of compounds in the nighttime (6 P.M. to midnight) compared to the morning (6 A.M. to noon) samples. The increased number of compounds in the 6 P.M. to midnight sample may indicate that nitrate radical chemistry was a source for these compounds, consistent with concurrent measurements of particulate peroxy nitrates by Rollins et al., which showed their concentrations increased during nighttime [*Rollins et al.*, 2012]. The distribution of the elemental ratios for the CHON compounds was different between the early morning (midnight to 6 A.M.) and the afternoon (noon to 6 P.M.) samples (Figures 3a and 3c). In the early morning (Figure 3a), the majority of the compounds had high O/C and H/C values, while in the afternoon (Figure 3c), many of those compounds were not observed and new compounds at lower O/C and H/C values appeared. This shift in composition is also shown in the decrease of the $<$O/C$>$ values from the early morning and morning to the afternoon and night samples (Table 1). The average O/C values for the N1 compounds show the same trends; they average between 0.67 and 0.70 in the early morning and morning (midnight–noon) and 0.59–0.60 in the afternoon and night (noon–midnight). These results are consistent with both the cessation of the formation of some of the higher O/C compounds, and the local production of new CHON compounds with lower O/C values in the afternoon formed through reactions of NO with organic peroxy radicals.

3.2.4. CHONS

Data for the CHONS compounds, shown in blue in Figure 3, fall in the same region of the van Krevelen diagram as the CHOS compounds and have on average slightly higher $<$O/C$>$ values (Figure 3 and Table 1). More than 80% of the CHONS compounds in each sample have enough oxygen atoms to have both sulfate and nitrate groups. The higher oxidation levels and the high numbers of oxygen atoms indicate that the majority of the CHONS compounds may be nitroxy organosulfates. The CHONS compounds covered a relatively narrow range of masses (300–400 Da) and they also had low relative intensities in these samples

Table 4. Nitroxy Organosulfate Compounds Detected With Both UPLC/MS and Nano-DESI/MS Analysis

		Concentration in ng/m^3 with UPLC/MS[a]			
Mass	Formula	20 June	21 June	22 June	23 June
295.0726	$C_{10}H_{16}N_1O_7S_1$	0.000 (a–d)	1.225 (b and d)	0.000 (a, c, and d)	0.000 (b and d)
297.0518	$C_9H_{14}N_1O_8S_1$	2.560 (a, b, and d)	7.306 (d)	3.313 (c)	1.880 (c)
311.0675	$C_{10}H_{16}N_1O_8S_1$	0.023 (a–d)	0.044 (a, b, and d)	0.009 (a–d)	0.000 (a–d)
313.0468	$C_9H_{14}N_1O_9S_1$	0.011 (a–d)	0.019 (a, b, and d)	0.022 (a–d)	0.055 (a–d)
327.0624	$C_{10}H_{16}N_1O_9S_1$	0.186 (a–d)	0.532 (a, b, and d)	0.090 (a–d)	0.000 (a–d)
329.078	$C_{10}H_{18}N_1O_9S_1$	0.008 (a–d)	0.025 (a, b, and d)	0.000 (a–d)	0.000 (a, b, and d)
331.0573	$C_9H_{16}N_1O_{10}S_1$	0.005 (a–d)	0.004 (a and b)	0.000 (a–d)	0.000 (a, b, and d)
343.0573	$C_{10}H_{16}N_1O_{10}S_1$	0.141 (a–d)	0.203 (a, b, and d)	0.081 (a–d)	0.380 (a–d)
374.0631[b]	$C_{10}H_{17}N_2O_{11}S_1$	0.685 (-)	0.274 (-)	0.076 (-)	0.377 (-)
390.058[b]	$C_{10}H_{17}N_2O_{12}S_1$	0.685 (b)	0.274 (-)	0.076 (-)	0.377 (a and b)
261.0155	$C_5H_{10}N_1O_9S_1$	0.000 (a and c)	0.027 (a, c, and d)	0.064 (a and b)	0.021 (a–c)
306.0005[b]	$C_5H_9N_2O_{11}S_1$	0.141 (-)	0.169 (-)	0.100 (-)	0.198 (1, c)

[a]These nitroxy organosulfates were also reported in *Surratt et al.* [2008]. The first number given is the concentration in ng/m^3 found with UPLC/MS and the letters in parenthesis correspond to the time of day the elemental formula was observed in the nano-DESI analysis (a = midnight to 6 A.M., b = 6 A.M. to noon, c = noon to 6 P.M., and d = 6 P.M. to midnight).
[b]Compounds observed only with UPLC/MS.

(Figure 1). The majority of the compounds had DBE values of 2–3 (Figure 2). These DBE values are in the same range as some of the CHONS compounds reported in fog water [*Mazzoleni et al.*, 2010]. The majority of the CHONS compounds contained N1, only 27 of the 142 unique CHONS compounds contained N2 or N3.

Between 32 and 70 CHONS compounds were observed, over the 4 day average, with more detected during the early morning and morning samples (midnight to 6 A.M. and 6 A.M. to noon) (Figure 1) than in the night sample (6 P.M. to midnight). The average percentage of CHONS compounds in the afternoon sample (noon to 6 P.M.) is also lower than the morning and early morning samples; however, it is just inside the standard deviation of the two morning samples. The greater numbers of compounds in the early morning and morning samples is consistent with a nitrate radical source for the nitrate part of the CHONS in the early morning and a slower, particle phase addition of sulfate. The lower numbers of CHONS compounds observed during the day indicate that either the formation mechanism is not as active later in the afternoon and night or there is a loss process for these compounds in the afternoon. Twelve of the CHONS compounds measured in these samples have elemental formulas corresponding to nitroxy organosulfates characterized by *Surratt et al.* [2008], which are formed from BVOCs, and are also measured by UPLC/MS analysis of 23 h integrated $PM_{2.5}$ filters (Table 4). The ion at *m/z* 296, which is likely derived from a limonene-like monoterpene [*Surratt et al.*, 2008], was the most abundant (9.7 ng m^{-3}) nitroxy organosulfates measured by the UPLC/MS technique. Like the organosulfates, the overlap between the two techniques was good; in 80% of the cases where a nitroxy organosulfate was reported using UPLC/MS, we observed a compound with the same molecular formula using nano-DESI/MS in at least one sample collected the same day. Given the lack of prior separation with nano-DESI/MS, it is likely that the compounds that were not observed with nano-DESI/MS, but that were seen with UPLC/MS, were lost because of charge competition in ESI. The larger number of CHONS compounds in the early morning and morning samples is consistent with local nighttime production of the compounds via nitrate radical chemistry. The overlap with some of the terpene-derived CHONS compounds identified using UPLC/MS indicates biogenic sources for some of these compounds.

As mentioned in the CHOS section, *Lin et al.* [2012b] also presented a method to investigate the prevalence of the epoxide formation pathway and the hydrolysis loss process for nitroxy organosulfates [*Lin et al.*, 2012b]. The number of reaction pairs, averaged over all four samples, for CHONS compounds are shown in the second and third columns of Table 3. Looking at the epoxide formation pathway (column 2), the percentage of CHONS compounds that had corresponding CHON plausible precursors ranged from ~30 to 40%. This is lower than the 40–80% seen for CHOS compounds indicating that this pathway is probably less significant for the CHONS compounds in Bakersfield. However, the range of values is higher than what was observed in China (0–15%) [*Lin et al.*, 2012b], which suggests a difference in formation mechanisms between the two locations. The third column of Table 3 shows the percentage of CHONS compounds that have a corresponding CHOS hydrolysis

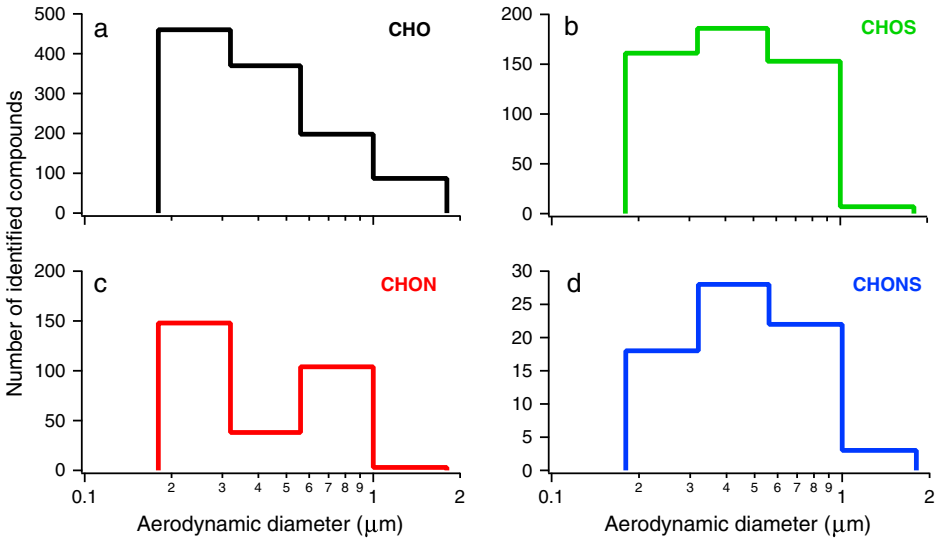

Figure 5. Number of CHO, CHOS, CHON, and CHONS compounds identified in four size-resolved samples collected by MOUDI (aerodynamic cutoff sizes 0.18, 0.32, 0.58, 1.0, and 1.8 μm) from the nano-DESI/MS analysis.

product in the sample. This reaction can occur in either the atmosphere or during sample preparation. Between ~66 and 80% of the CHONS compounds had the corresponding CHOS product in the sample. These values are in the same range as the results from China [*Lin et al.*, 2012b] and indicate that hydrolysis is likely a major loss process for the nitroxy organosulfates in these samples.

3.3. Characterization of Organics in Size-Resolved Samples

Size-resolved data were analyzed for the 12 h samples collected on 24 June from noon to midnight. The total number of compounds decreased from stage 8 to stage 5 with 787 compounds on stage 8 (0.18–0.32 μm), 622 on stage 7 (0.32–0.56 μm), 477 on stage 6 (0.56–1.0 μm), and 100 on stage 5 (1.0–1.8 μm). This trend follows the decrease in mass loadings of organics in increasing size fractions that was seen on 22 and 23 June [*O'Brien et al.*, 2013a]. The data were separated into the same four groups: CHO, CHOS, CHON, and CHONS. Figure 5 shows the number of identified compounds for each group, as a function of the aerodynamic diameter cut-points for each MOUDI stage. The CHO compounds showed a gradual decrease in the number of compounds detected in the samples of larger size fractions. In contrast, the number of CHOS and CHONS compounds increased slightly on stage 7 (0.32–0.56 μm) and then decreased slightly on stage 6 (0.56–1.0 μm). The size ranges observed for the CHOS compounds are consistent with results showing the highest concentrations of organosulfates below one micron [*Lukacs et al.*, 2009; *Hatch et al.*, 2011]. These results indicate that the eighth stage contained the largest number of organic compounds (CHO) and that the two sulfur-containing groups have roughly equal numbers of compounds observed across these size ranges.

Figure 6 shows van Krevelen diagrams for the data in each sample and the intensity weighted average elemental ratios for each group are given in Table S7. The range of elemental ratios for the CHO, CHOS, and CHONS groups were similar across the bottom three stages of the MOUDI (stages 8–6: (0.18–0.32 μm), (0.32–0.56 μm), (0.56–1.0 μm). All three groups fall in similar ranges in the Van Krevelen diagrams as the samples discussed previously. This is consistent with the majority of the compounds having sulfur and nitrogen in sulfate and nitrate groups.

The CHON compounds showed different behavior as the aerosol size increased. From stage 8 (0.18-0.32 μm) to stage 7(0.32–0.56 μm), there was a large decrease in the number of CHON compounds. Most of the CHON compounds at higher O/C values in the stage 8 sample were not observed in the stage 7 sample and thus, the $<$O/C$>$ of the CHON compounds decreased on stage 7. For stage 6 (0.56–1.0 μm), the number of CHON compounds almost tripled compared to stage 7, increasing to 105 (Figure 5). The majority (97%) of the CHON compounds on stage 8 had O/N values $>$3 consistent with organonitrates. However, many of the CHON compounds on stage 6 were located at lower H:C values than the CHON compounds on stage 8 (Figure 6).

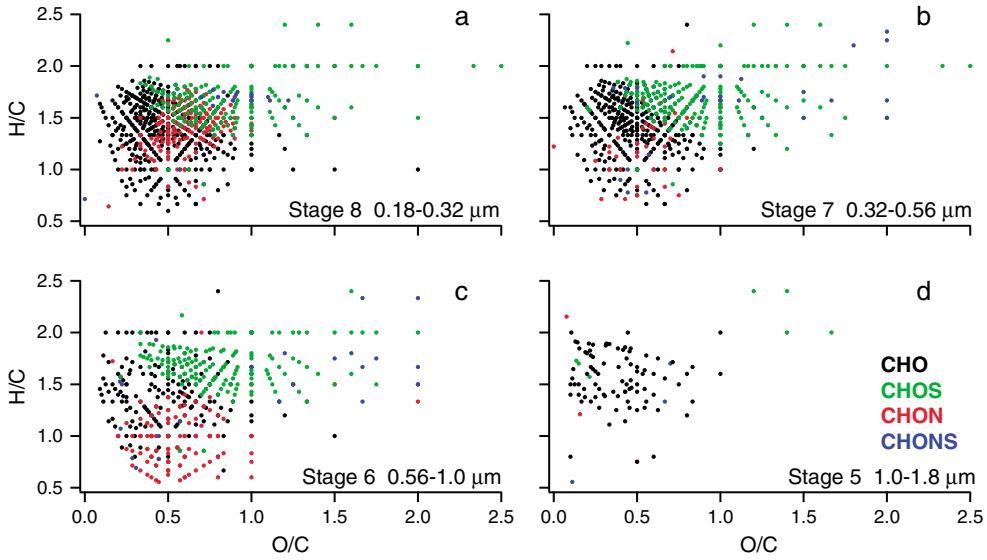

Figure 6. Van Krevelen diagrams showing the elemental ratios for the samples from MOUDI stages 8–5 (a–d) ($0.18 < D_a < 1.8$ μm) from the nano-DESI/MS analysis.

The<N/C> values for the stage 6 CHON compounds were higher (0.30 versus 0.08 on stage 8) and at least 50% of them did not have enough oxygen atoms in the molecular formula for all of the nitrogen atoms to be organic nitrate (ONO_2) groups. Additionally, the AI values for 33 of them were ≥0.67 indicating the presence of condensed aromatic compounds. These results suggest that some of the CHON compounds in the $0.56 < D_a < 1.0$ μm size fraction were aromatic compounds with nitrogen atoms in the rings and nitroaromatic compounds which can be formed through the photooxidation of aromatic compounds in the presence of NO_x [*Forstner et al.*, 1997; *Wozniak et al.*, 2008]. The CHON group shows a large change from the accumulation mode to the droplet mode and further work analyzing the chemical composition of aerosols in size-resolved fractions is needed to provide information on the sources of these compounds.

4. Conclusions

The molecular composition of atmospheric particulate matter collected during the CalNex 2010 campaign in Bakersfield, California was investigated using negative ion mode nano-DESI/MS and UPLC/MS. With nano-DESI/MS, approximately 600–900 compounds were identified in the mass range of 50–400 Da for each sample. Four groups of compounds were identified: compounds that contained carbon, hydrogen, and oxygen (CHO), nitrogen containing (CHON), sulfur containing (CHOS), and nitrogen and sulfur containing (CHONS). The molecular formulas for these compounds were consistent with organonitrates, organosulfates, and nitroxy organosulfates, respectively.

Changes were observed in the molecular composition throughout the day consistent with daytime production of CHO and CHON compounds. Similar results were observed for CHO compounds using positive ion mode nano-DESI/MS [*O'Brien et al.*, 2013a], and thus, photochemistry and ozonolysis are likely sources for the full range (both positive and negative ion mode) of CHO compounds measured in Bakersfield. Increases in the number of nitrogen-containing compounds in the night and early morning samples are consistent with nighttime production of CHON and CHONS compounds, likely through nitrate radical chemistry. Positive ion mode nano-DESI/MS [*O'Brien et al.*, 2013a] also showed increased numbers of CHON compounds in night samples; however, many of those molecular formula were consistent with imidization formation reactions. Thus, in Bakersfield, both imidization reactions and nitrate radical chemistry likely contribute to the number of nitrogen-containing compounds in organic aerosols. The CHOS compounds were observed only in the negative mode and had the smallest change in the number of compounds measured in each sample, consistent with a more remote source, and had precursor-product pairs consistent with an epoxide formation on biogenic precursors. The trends observed in all of these data sets are for a small number of days (2–4) and, thus, a larger data set is necessary to identify the statistical significance of these trends. Additionally, the

observed changes are consistent with the previously discussed processes, however, other sources and formation mechanisms for these compounds likely also contribute.

Using size-resolved samples, the number of CHON compounds was found to be bimodal. The smaller size fraction ($0.18 < D_a < 0.32\ \mu m$) had molecular formulas consistent with organonitrates while the larger size fraction ($0.56 < D_a < 1.0\ \mu m$) likely contained aromatic compounds with nitrogen atoms in the rings and nitroaromatic compounds.

The overlap in molecular formulas with identified organosulfates and nitroxy organosulfates from SOA formed from BVOC sources is consistent with a biogenic source for some of the compounds measured in Bakersfield. Additionally, the presence of organosulfates, organonitrates, and nitroxy organosulfates observed here as well as the previously observed larger overlap between ambient SOA and diesel SOA [*O'Brien et al.,* 2013b] are both consistent with anthropogenic sources for compounds measured in Bakersfield. The changes observed in the chemical composition during the day in both these data sets and those in *O'Brien et al.* [2013a] suggest some local processing of SOA while the smaller changes in the CHOS percentages through the day suggest a more remote source for those compounds. Thus, atmospheric organic aerosols in Bakersfield showed evidence of both local and longer range transport of SOA from both biogenic and anthropogenic sources.

Good overlap was observed between the two techniques: 97% and 80% of the time an organosulfate or nitroxy organosulfate, respectively, was measured with negative ion mode UPLC/MS, a compound with the same molecular formula was detected with negative ion mode nano-DESI/MS on the same day. The agreement between the two techniques demonstrates the utility of combining these analysis methods to provide both a highly sensitive measure of the ionizable fraction of the chemical composition using nano-DESI HR-MS as well as chemical identification and quantitation of selected compounds using UPLC/MS.

Acknowledgments

Data supporting Figures 1–3 are available in Table S8 in the supporting information. The UC group acknowledges support from the California Air Resources Board under contracts 08-316 and 09-316. A.L. acknowledges support from NOAA Climate Program Office's AC4 program, award NA13OAR4310066. J.L. acknowledges support from the Chemical Sciences Division, Office of Basic Energy Sciences (BES) of the U.S. DOE. The nano-DESI/MS experiments described in this paper were performed in the Environmental Molecular Sciences Laboratory, a national scientific user facility sponsored by OBER U.S. DOE and located at the Pacific Northwest National Laboratory (PNNL). PNNL is operated for US DOE by Battelle Memorial Institute under Contract No. DE-AC06-76RL0 1830. The UNC group acknowledges support from Alion Science and Technology under contract EP-D-05-065 in order to collect $PM_{2.5}$ samples at the Bakersfield ground site. C.L.R. acknowledges support from the Weiss Urban Livability Fellowship and Johanssen Scholarship programs at UNC, as well as from the Electric Power Research Institute (EPRI). UPLC/ESI-HR-Q-TOFMS analyses were conducted in the UNC Biomarker Mass Facility located within the Department of Environmental Sciences and Engineering, which is a part of the UNC Center for Environmental Health and Susceptibility and is supported by NIEHS (grant 5P20-ES10126). The authors would like thank Nathan Kreisberg for help in the development and implementation of the sampling setup and John Offenburg at the EPA for the use of the MOUDI samplers. We would also like to thank John Karlik, Ron Cohen, Sally Pusede, University of California Extension Staff, and Kern County Staff, for logistical support during the Bakersfield CALNEX study.

References

Altieri, K. E., B. J. Turpin, and S. P. Seitzinger (2009), Oligomers, organosulfates, and nitrooxy organosulfates in rainwater identified by ultra-high resolution electrospray ionization FT-ICR mass spectrometry, *Atmos. Chem. Phys.*, *9*(7), 2533–2542.

Bateman, A. P., S. A. Nizkorodov, J. Laskin, and A. Laskin (2009), Time-resolved molecular characterization of limonene/ozone aerosol using high-resolution electrospray ionization mass spectrometry, *Phys. Chem. Chem. Phys.*, *11*(36), 7931–7942.

Claeys, M., R. Vermeylen, F. Yasmeen, Y. Gómez-González, X. G. Chi, W. Maenhaut, T. Meszaros, and I. Salma (2012), Chemical characterisation of humic-like substances from urban, rural and tropical biomass burning environments using liquid chromatography with UV/vis photodiode array detection and electrospray ionisation mass spectrometry, *Environ. Chem.*, *9*(3), 273–284.

Duffin, K. L., J. D. Henion, and J. J. Shieh (1991), Electrospray and tandem mass-spectrometric characterization of acylglycerol mixtures that are dissolved in nonpolar-solvents, *Anal. Chem.*, *63*(17), 1781–1788.

Ervens, B., B. J. Turpin, and R. J. Weber (2011), Secondary organic aerosol formation in cloud droplets and aqueous particles (aqSOA): A review of laboratory, field and model studies, *Atmos. Chem. Phys.*, *11*(21), 11,069–11,102.

Fenn, J. B., M. Mann, C. K. Meng, S. F. Wong, and C. M. Whitehouse (1990), Electrospray ionization-principles and practice, *Mass Spectrom. Rev.*, *9*(1), 37–70.

Forstner, H. J. L., R. C. Flagan, and J. H. Seinfeld (1997), Secondary organic aerosol from the photooxidation of aromatic hydrocarbons: Molecular composition, *Environ. Sci. Technol.*, *31*(5), 1345–1358.

Fuzzi, S., et al. (2006), Critical assessment of the current state of scientific knowledge, terminology, and research needs concerning the role of organic aerosols in the atmosphere, climate, and global change, *Atmos. Chem. Phys.*, *6*, 2017–2038.

Gong, H. M., A. Matsunaga, and P. J. Ziemann (2005), Products and mechanism of secondary organic aerosol formation from reactions of linear alkenes with NO3 radicals, *J. Phys. Chem. A*, *109*(19), 4312–4324.

Hatch, L. E., J. M. Creamean, A. P. Ault, J. D. Surratt, M. N. Chan, J. H. Seinfeld, E. S. Edgerton, Y. Su, and K. A. Prather (2011), Measurements of isoprene-derived organosulfates in ambient aerosols by aerosol time-of-flight mass spectrometry—Part 1: Single particle atmospheric observations in Atlanta, *Environ. Sci. Technol.*, *45*(12), 5105–5111.

Havers, N., P. Burba, J. Lambert, and D. Klockow (1998), Spectroscopic characterization of humic-like substances in airborne particulate matter, *J. Atmos. Chem.*, *29*(1), 45–54.

Holzinger, R., A. Kasper-Giebl, M. Staudinger, G. Schauer, and T. Röckmann (2010), Analysis of the chemical composition of organic aerosol at the Mt. Sonnblick observatory using a novel high mass resolution thermal-desorption proton-transfer-reaction mass-spectrometer (hr-TD-PTR-MS), *Atmos. Chem. Phys.*, *10*(20), 10,111–10,128.

Iinuma, Y., O. Boge, A. Kahnt, and H. Herrmann (2009), Laboratory chamber studies on the formation of organosulfates from reactive uptake of monoterpene oxides, *Phys. Chem. Chem. Phys.*, *11*(36), 7985–7997.

Kalberer, M. (2006), Analysis of oligomers in atmospheric aerosol particles—Analytical challenges, *Anal. Bioanal. Chem.*, *385*(1), 22–25.

Kanakidou, M., et al. (2005), Organic aerosol and global climate modelling: A review, *Atmos. Chem. Phys.*, *5*, 1053–1123.

Kendrick, E. (1963), A mass scale based on Ch2 = 14.0000 for high resolution mass spectrometry of organic compounds, *Anal. Chem.*, *35*(13), 2146–2154.

Koch, B. P., and T. Dittmar (2006), From mass to structure: An aromaticity index for high-resolution mass data of natural organic matter, *Rapid Commun. Mass Spectrom.*, *20*(5), 926–932.

Kourtchev, I., S. Fuller, J. Aalto, T. M. Ruuskanen, M. W. McLeod, W. Maenhaut, R. Jones, M. Kulmala, and M. Kalberer (2013), Molecular composition of boreal forest aerosol from Hyytiala, Finland, using ultrahigh resolution mass spectrometry, *Environ. Sci. Technol.*, *47*(9), 4069–4079.

Laskin, A., J. S. Smith, and J. Laskin (2009), Molecular characterization of nitrogen-containing organic compounds in biomass burning aerosols using high-resolution mass spectrometry, *Environ. Sci. Technol.*, *43*(10), 3764–3771.

Laskin, A., J. Laskin, and S. A. Nizkorodov (2012), Mass spectrometric approaches for chemical characterisation of atmospheric aerosols: Critical review of the most recent advances, *Environ. Chem.*, *9*(3), 163–189.
Laskin, J., A. Laskin, P. J. Roach, G. W. Slysz, G. A. Anderson, S. A. Nizkorodov, D. L. Bones, and L. Q. Nguyen (2010), High-resolution desorption electrospray ionization mass spectrometry for chemical characterization of organic aerosols, *Anal. Chem.*, *82*(5), 2048–2058.
Lin, P., A. G. Rincon, M. Kalberer, and J. Z. Yu (2012a), Elemental composition of HULIS in the Pearl River Delta Region, China: Results inferred from positive and negative electrospray high resolution mass spectrometric data, *Environ. Sci. Technol.*, *46*(14), 7454–7462.
Lin, P., J. Z. Yu, G. Engling, and M. Kalberer (2012b), Organosulfates in Humic-like substance fraction isolated from aerosols at seven locations in East Asia: A study by ultra-high-resolution mass spectrometry, *Environ. Sci. Technol.*, *46*(24), 13,118–13,127.
Lin, Y.-H., et al. (2012), Isoprene epoxydiols as precursors to secondary organic aerosol formation: Acid-catalyzed reactive uptake studies with authentic compounds, *Environ. Sci. Technol.*, *46*(1), 250–258.
Lin, Y.-H., E. M. Knipping, E. S. Edgerton, S. L. Shaw, and J. D. Surratt (2013), Investigating the influences of SO_2 and NH_3 levels on isoprene-derived secondary organic aerosol formation using conditional sampling approaches, *Atmos. Chem. Phys.*, *13*(16), 8457–8470.
Lukacs, H., A. Gelencsér, A. Hoffer, G. Kiss, K. Horváth, and Z. Hartyáni (2009), Quantitative assessment of organosulfates in size-segregated rural fine aerosol, *Atmos. Chem. Phys.*, *9*(1), 231–238.
Mazzoleni, L. R., B. M. Ehrmann, X. Shen, A. G. Marshall, and J. L. Collett Jr. (2010), Water-soluble atmospheric organic matter in fog: Exact masses and chemical formula identification by ultrahigh-resolution fourier transform ion cyclotron resonance mass spectrometry, *Environ. Sci. Technol.*, *44*(10), 3690–3697.
Ng, N. L., et al. (2008), Secondary organic aerosol (SOA) formation from reaction of isoprene with nitrate radicals (NO(3)), *Atmos. Chem. Phys.*, *8*(14), 4117–4140.
Nguyen, T. B., A. P. Bateman, S. A. Nizkorodov, J. Laskin, and A. Laskin (2010), High-resolution mass spectrometry analysis of secondary organic aerosol generated by ozonolysis of isoprene, *Atmos. Environ.*, *44*(8), 1032–1042.
Nguyen, T. B., A. Laskin, J. Laskin, and S. A. Nizkorodov (2012), Direct aqueous photochemistry of isoprene high-NOx secondary organic aerosol, *Phys. Chem. Chem. Phys.*, *14*(27), 9702–9714.
Nizkorodov, S. A., J. Laskin, and A. Laskin (2011), Molecular chemistry of organic aerosols through the application of high resolution mass spectrometry, *Phys. Chem. Chem. Phys.*, *13*(9), 3612–3629.
Noziere, B., S. Ekstrom, T. Alsberg, and S. Holmstrom (2010), Radical-initiated formation of organosulfates and surfactants in atmospheric aerosols, *Geophys. Res. Lett.*, *37*, L05806, doi:10.1029/2009GL041683
O'Brien, R. E., A. Laskin, J. Laskin, S. Liu, R. Weber, L. M. Russell, and A. H. Goldstein (2013a), Molecular characterization of organic aerosol using nanospray desorption/electrospray ionization mass spectrometry: CalNex 2010 field study, *Atmos. Environ.*, *68*, 265–272.
O'Brien, R. E., T. B. Nguyen, A. Laskin, J. Laskin, P. L. Hayes, S. Liu, J. L. Jimenez, L. M. Russell, S. A. Nizkorodov, and A. H. Goldstein (2013b), Probing molecular associations of field-collected and laboratory-generated SOA with nano-DESI high-resolution mass spectrometry, *J. Geophys. Res. Atmos.*, *118*, 1042–1051, doi:10.1002/jgrd.50119.
Poschl, U. (2005), Atmospheric aerosols: Composition, transformation, climate and health effects, *Angew. Chem. Int. Ed.*, *44*(46), 7520–7540.
Reemtsma, T., A. These, P. Venkatachari, X. Xia, P. K. Hopke, A. Springer, and M. Linscheid (2006), Identification of fulvic acids and sulfated and nitrated analogues in atmospheric aerosol by electrospray ionization Fourier transform ion cyclotron resonance mass spectrometry, *Anal. Chem.*, *78*(24), 8299–8304.
Roach, P. J., J. Laskin, and A. Laskin (2010a), Molecular characterization of organic aerosols using Nanospray-Desorption/Electrospray Ionization-Mass Spectrometry, *Anal. Chem.*, *82*(19), 7979–7986.
Roach, P. J., J. Laskin, and A. Laskin (2010b), Nanospray desorption electrospray ionization: An ambient method for liquid-extraction surface sampling in mass spectrometry, *Analyst*, *135*(9), 2233–2236.
Roach, P. J., J. Laskin, and A. Laskin (2011), Higher-order mass defect analysis for mass spectra of complex organic mixtures, *Anal. Chem.*, *83*(12), 4924–4929.
Roberts, J. M. (1990), The atmospheric chemistry of organic nitrates, *Atmos. Environ. Gen. Top.*, *24*(2), 243–287.
Rogge, W. F., M. A. Mazurek, L. M. Hildemann, G. R. Cass, and B. R. T. Simoneit (1993), Quantification of urban organic aerosols at a molecular-level—Identification, abundance and seasonal-variation, *Atmos. Environ. Gen. Top.*, *27*(8), 1309–1330.
Rollins, A. W., et al. (2012), Evidence for NOx control over nighttime SOA formation, *Science*, *337*(6099), 1210–1212.
Samburova, V., R. Zenobi, and M. Kalberer (2005), Characterization of high molecular weight compounds in urban atmospheric particles, *Atmos. Chem. Phys.*, *5*, 2163–2170.
Seinfeld, J. H., and J. F. Pankow (2003), Organic atmospheric particulate material, *Annu. Rev. Phys. Chem.*, *54*, 121–140.
Solomon, S., D. Qin, M. Manning, Z. Chen, M. Marquis, K. B. Averyt, M. Tignor, and H. L. Miller (Eds.) (2007), Contribution of working group I to the fourth assessment report of the Intergovernmental Panel on Climate Change, in *IPCC, 2007: Climate Change 2007: The Physical Science Basis*, Cambridge Univ. Press, Cambridge, U. K., and New York.
Surratt, J. D., et al. (2008), Organosulfate formation in biogenic secondary organic aerosol, *J. Phys. Chem. A*, *112*(36), 8345–8378.
Surratt, J. D., A. W. Chan, N. C. Eddingsaas, M. Chan, C. L. Loza, A. J. Kwan, S. P. Hersey, R. C. Flagan, P. O. Wennberg, and J. H. Seinfeld (2010), Reactive intermediates revealed in secondary organic aerosol formation from isoprene, *Proc. Natl. Acad. Sci. U.S.A.*, *107*(15), 6640–6645.
Williams, B. J., A. H. Goldstein, N. M. Kreisberg, S. V. Hering, D. R. Worsnop, I. M. Ulbrich, K. S. Docherty, and J. L. Jimenez (2010), Major components of atmospheric organic aerosol in southern California as determined by hourly measurements of source marker compounds, *Atmos. Chem. Phys.*, *10*(23), 11,577–11,603.
Wozniak, A. S., J. E. Bauer, R. L. Sleighter, R. M. Dickhut, and P. G. Hatcher (2008), Technical Note: Molecular characterization of aerosol-derived water soluble organic carbon using ultrahigh resolution electrospray ionization Fourier transform ion cyclotron resonance mass spectrometry, *Atmos. Chem. Phys.*, *8*(17), 5099–5111.
Zhang, H. F., et al. (2012), Organosulfates as tracers for secondary organic aerosol (SOA) formation from 2-Methyl-3-Buten-2-ol (MBO) in the atmosphere, *Environ. Sci. Technol.*, *46*(17), 9437–9446.
Zhang, H., J. D. Surratt, Y. H. Lin, J. Bapat, and R. M. Kamens (2011), Effect of relative humidity on SOA formation from isoprene/NO photooxidation: Enhancement of 2-methylglyceric acid and its corresponding oligoesters under dry conditions, *Atmos. Chem. Phys.*, *11*(13), 6411–6424.
Zhang, Q., C. Anastasio, and M. Jimemez-Cruz (2002), Water-soluble organic nitrogen in atmospheric fine particles (PM2.5) from northern California, *J. Geophys. Res.*, *107*(D11), 4112, doi:10.1029/2001JD000870.
Zhang, Q., et al. (2007), Ubiquity and dominance of oxygenated species in organic aerosols in anthropogenically-influenced Northern Hemisphere midlatitudes, *Geophys. Res. Lett.*, *34*, L13801, doi:10.1029/12007GL029979.